metals

MDPI

Review

Microstructure and Mechanical Properties of Titanium Alloys Produced by Additive Technologies: New Approaches and Promising Areas of Research

Irina P. Semenova [1,*], Alexander V. Polyakov [1], Yuecheng Dong [2], Zhonggang Sun [2] and Igor V. Alexandrov [1]

[1] Department of Materials Science and Metal Physics, Ufa University of Science and Technology, 32 Zaki Validi St., 450076 Ufa, Russia; alex-v.polyakov@mail.ru (A.V.P.); igorvalexandrov@yandex.ru (I.V.A.)
[2] College of Materials Science and Engineering/Tech Institute for Advanced Materials, Nanjing Tech University, Nanjing 211816, China; dongyuecheng@njtech.edu.cn (Y.D.); sunzgg@njtech.edu.cn (Z.S.)
* Correspondence: semenova-ip@mail.ru

Abstract: Additive manufacturing, or 3D printing, is a process where a part is produced layer by layer, and represents a promising approach for designing components close to their final shape. Titanium alloys produced by additive manufacturing find application in various industries. This overview examines the features of the formation of the microstructure and properties in Ti alloys synthesized with the use of powder and wire laser additive technologies, as well as solid-phase methods of additive manufacturing such as friction stir additive manufacturing. Their main drawbacks and advantages are discussed, as applied to Ti alloys. The main approaches to solving the problem of increasing the strength properties of the synthesized Ti workpieces are considered. The authors of this overview propose a new area of research in the field of the application of additive technologies for producing ultrafine-grained Ti semi-products and parts with enhanced performance characteristics. Research in this area opens up prospects for designing heavily loaded complex-profile products for the aerospace, oil and gas, and biomedical industries.

Keywords: titanium alloys; additive manufacturing; microstructure; mechanical properties; nanostructure; ultrafine-grained structure

Citation: Semenova, I.P.; Polyakov, A.V.; Dong, Y.; Sun, Z.; Alexandrov, I.V. Microstructure and Mechanical Properties of Titanium Alloys Produced by Additive Technologies: New Approaches and Promising Areas of Research. *Metals* **2024**, *14*, 966. https://doi.org/10.3390/met14090966

Academic Editor: Dariusz Rozumek

Received: 25 July 2024
Revised: 20 August 2024
Accepted: 22 August 2024
Published: 27 August 2024

1. Introduction

Titanium alloys are widely used in various industries, in particular, in medicine and aviation due to their high specific strength and corrosion resistance [1–3]. In modern conditions, the production of titanium semi-products and products using traditional forging, die forging, and casting technologies requires significant costs for production planning. The use of additive manufacturing enables the acceleration of the solution of technological problems and reduces the cost of producing finished products. The additive manufacturing of titanium alloy parts can provide estimated production savings of up to 50%, effectively reducing exorbitant processing costs and material waste [4–8].

For materials synthesized using powder and wire additive technologies, the metal is subjected to the repeated processes of melting and solidification. They often have problems such as residual stresses, a rough dendritic structure, anisotropy of properties, and porosity [4–6]. Additive manufacturing methods based on friction welding have certain advantages over conventional 3D printing methods, since the process occurs in the solid-phase state. One can note the absence of porosity in the finished part, a good balance of mechanical properties and a low level of residual stresses [9–12]. Friction stir additive manufacturing (FSAM) is an innovative process for producing complex-profile parts for the aerospace industry [11]. Technically, this involves applying pressure to a specially designed welding tool that is rotated at high spindle speed between two joined sheets and is then moved along the joint line. The frictional heat and plastic deformation

caused by the rotating tool increase the local temperature of the material being welded, so it can be plastically deformed under relatively little stress. Thus, the material being welded is subjected to very large degrees of deformation at high strain rates and elevated temperatures. This process is already used for aluminum alloys and steels [13,14]. In recent decades, a large number of studies have appeared in the field of the friction welding of titanium alloys. However, the welding of titanium alloys using the FSAM method is a significantly more difficult process compared to aluminum alloys due to the high reactivity of titanium, as well as increased requirements for the tools [15].

In the second section of this overview, most attention is paid to the features of microstructure formation in titanium α, α + β, and β alloys synthesized by additive manufacturing. A large number of publications and overviews are devoted to the study of the microstructure and properties of titanium alloys in the process of the laser sintering of powder or wire. Considering the fact that the material undergoes melting and solidification during each deposition cycle, the microstructure of the synthesized workpieces is close to cast and is characterized by a large lamellar structure. Section 3 shows that the use of additive technologies based on friction welding or solid-phase additive technologies due to local heating in the contact zone in combination with deformation leads to the formation of more complex microstructures of the weld, as reported in the publications of various researchers. Section 4 discusses the mechanical properties achieved to date in Ti alloys synthesized by different methods. Research over the past 10–15 years has shown that the main efforts in the field of producing titanium alloys using additive manufacturing are aimed at increasing their mechanical properties by refining the microstructure in the weld during the laser sintering of powders and wires, as well as achieving an equiaxed α-structure, up to an ultrafine-grained structure, in the additive manufacture of titanium workpieces based on friction welding. Some results in these areas of research are discussed in Section 5 of this overview.

One of the new areas of research in the field of additive technologies is the production of parts and products with an ultrafine-grained (UFG) structure. It is known [16] that reducing the grain size in metals to values in the range of 0.1–1.0 μm using severe plastic deformation (SPD) processing leads to the significant strengthening of the material due to an increase in the length of grain boundaries and an increase in dislocation density, i.e., the involvement of the grain boundary and dislocation strengthening mechanisms. The use of initial materials with an ultrafine-grained structure in the process of the additive manufacturing of semi-products, for example, using FSAM, can lead to a synergistic effect of the enhancement of the material's mechanical properties due to the preservation of ultrafine grains and the implementation of high strain rate and/or low-temperature superplasticity in the contact zone, which leads to an orderly flow of material. Research in this area aimed at increasing the performance properties of titanium alloys opens up prospects for designing highly loaded products with complex profiles for the aerospace, oil and gas, and biomedical industries.

2. Microstructure and Properties of Titanium Alloys Synthesized Using Additive Manufacturing by the Melting of Powder/Wire

2.1. Ti and the Ti-6Al-4V Alloy

For materials synthesized using powder and wire additive technologies, the metal is subjected to the repeated processes of melting and solidification [6]. The most popular technologies of additive manufacturing (AM) for the production of parts from a Ti alloy are electron beam melting (EBM), selective laser melting (SLM), and directed energy deposition (DED), investigated in many critical overviews [3,17–21].

In an overview, the authors of [22] analyzed the advantages of additive technologies in relation to titanium alloys for use in biomedicine. In particular, the microstructural features of commercially pure (CP) Ti vary from lamellar α- to needle-like martensitic α'-phases, depending on the SLM mode. This difference in microstructure can be explained by different laser processing parameters, especially scanning speed. Mechanical properties

such as tension, compression, and the hardness of SLM-fabricated CP Ti samples indicate that SLM is able to produce samples with superior properties compared to conventional deformation processing or casting. For example, the yield strength and the ultimate tensile strength (UTS) of SLM-produced CP Ti are 555 and 757 MPa, respectively, which are higher than those in sheet forming. In addition, the Vickers microhardness of the CP Ti samples is higher than that produced by traditional casting and is comparable with cold-rolled CP Ti. This noticeable hardening may be due to grain refinement at high cooling rates during SLM processing.

The UTS of the Ti-6Al-4V alloy produced by SLM can reach 1300 MPa compared to cast billets that have a strength of approximately 850 MPa. This improvement in mechanical properties can be attributed to the martensitic microstructure that results from the SLM treatment [22].

Laser powder bed fusion (LPBF) is a relevant and important additive manufacturing technology that offers plenty of opportunities for the production of three-dimensional complex components with a high resolution and short execution times. This technology is applied when manufacturing parts for the aerospace and biomedical industries. However, there are still many problems, including poor surface quality, porosity, and the anisotropy of microstructure and properties, as well as the difficulty of microstructure adaptation [21]. It was demonstrated in an overview [19] that microstructure is influenced by the highest generated temperature and cooling rate that may be adjusted using the input variable AM processes.

Typical microstructures of the Ti-6Al-4V alloys produced by different AM processes are shown in Figure 1.

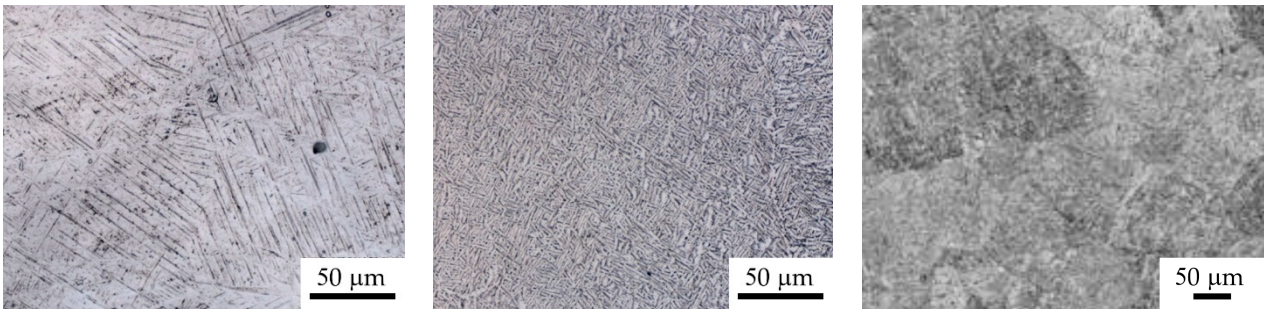

(**a**) (**b**) (**c**)

Figure 1. As-built microstructures of a Ti-6Al-4V parts produced by (**a**) SLM Reprinted with permission from ref. [23]. 2016 Springer Nature, (**b**) EBM [23], and (**c**) DED [24] processes.

In all cases, these are microstructures of the α + β type, with a prevailing martensitic structure. The originally molten bath cools rapidly, and during crystallization a phase transformation of the β-phase into martensite occurs. Then the temperature remains relatively constant in a range of assembly temperatures, approximately 600–760 °C, until the deposition process is complete. At this stage, the high assembly temperature of the EBM process acts as an incomplete heat treatment leading to martensite breakdown with the formation of an (α + β) lamellar structure. A certain amount of martensite may remain in the microstructure (Figure 1b).

In [25], selective laser melting and electron beam melting are discussed from the perspective of raw material production and processing–microstructure relationships. For the control of the PBF processes, an overview is presented, covering approaches to computer simulation for the imitation of the process parameters and defects, such as residual stresses and porosity in different length scales. A conclusion is made that, through improving the methods of powder production, new alloy design, and further development of the ALM equipment, the PBF methods may reach commercial maturity.

In this section, more attention will be given to additive technologies based on layer-by-layer wire welding deposition that have been developed in the last decade [26].

Used as heat sources in additive manufacturing are arc electrodes (WAAM) [8,27], laser powder based fusion (LPBF), and electron beam welding [7,8]. When using wire additive manufacturing methods, after cooling, the microstructure of the product consists of a large number of columnar dendrites and a coarse lamellar structure in the primary β-grains (Figure 2). Such a heterogeneous microstructure over the cross-section of the resulting workpiece subsequently influences the final mechanical properties of the synthesized material [8].

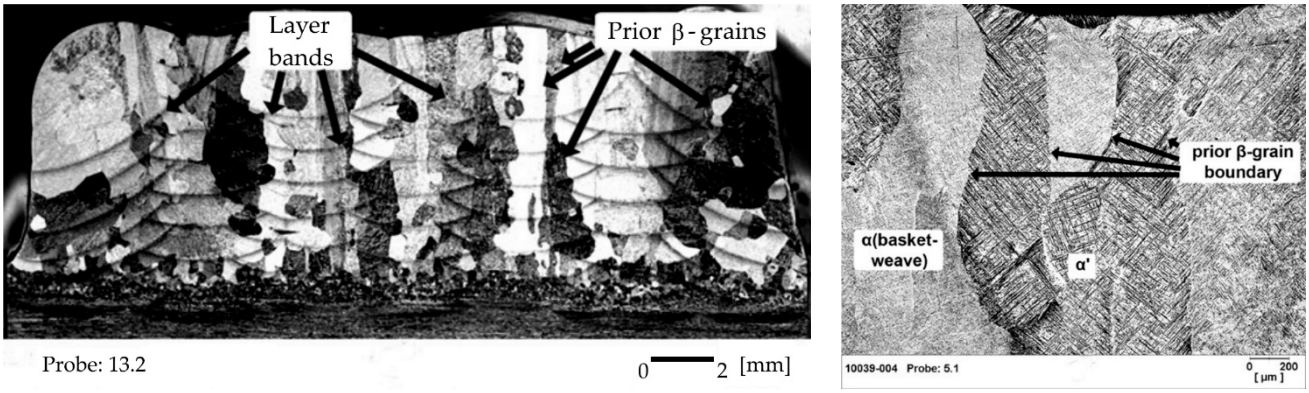

(**a**) (**b**)

Figure 2. Macrostructure (**a**) and microstructure (**b**) of the Ti-6Al-4 V alloy produced by layer-by-layer wire deposition [28].

By using wire filler material compared to powder-based manufacturing processes, arc additive manufacturing offers higher deposition productivity as well as increased metal utilization. Moreover, the generally lower contamination of welding wire compared to powder is also an advantage in terms of material quality. Wire-based technologies, as opposed to powder-based ones, appear to provide a higher level of reproducibility due to their ease of setup and process operation, as well as higher deposition rates [8].

A large number of studies in the field of additive technologies using wire are devoted to various series of steels [27,29]. However, experience and developments in the production of titanium alloy wire-based products are relatively limited to date. Therefore, the activity of researchers in this area is currently growing. In particular, publications report the use of the method of layer-by-layer Ti-6Al-4V alloy wire deposition using a high-power diode laser [28,30,31] that makes it possible to produce synthesized workpieces with a hardness of approximately 340 HV, which is about 15–30% lower than the hardness of the monolithic alloy. Due to the high anisotropy of the forming dendritic coarse-grained (CG) structure, the ultimate tensile strength (UTS) of such workpieces made of the Ti-6Al-4V alloy is usually about 940 MPa across the wall building direction, and about 1000 MPa along the wall building direction [30], in contrast to die-forged workpieces, the UTS of which can reach 1100 MPa [32].

As known, the strength properties of titanium and its alloys depend on the morphology of the α-phase and the sizes of the β-grains, which vary depending on the temperature and heating rate of the material, as well as the cooling rate [33]. Obviously, the lower the heat input during the deposition, the higher the heating and cooling rates; the smaller the β-grain size, the higher the volume fraction of the "harder" α-phase, and the higher the hardness of the synthesized alloy [31]. This is also reported in works that present the results of studies on the selection of the parameters of laser deposition with wire feed [34].

In [35], the experimental results for the Ti-6Al-4V alloy synthesized by WAAM confirm, when correctly selecting the WAAM process parameters, that it is possible to achieve mechanical properties very close to those traditional for the Ti-6Al-4V alloy. In particular, it was demonstrated that the wire feed rate had a greater effect on the weld geometry than the welding rate. An epitaxial growth of the primary β-grains in several layers and

graduated microstructure in the state after printing were observed. Owing to the rapid cooling, during the compression tests the strength values of 884 MPa for 0.2% compression and 1031 MPa for 2% compression were achieved. The STA heat treatment led to a decrease in mechanical strength, which was attributed to the coarsened microstructural change to a fully equiaxed microstructure.

Compared to other melting sources, WAAM provides a considerable cost saving and a higher deposition rate. The paper [36] provides a comprehensive overview of the literature on WAAM, including the stage-by-stage development of WAAM, the used metals and alloys, and the effect of the process parameters. The main problems occurring during WAAM, such as undesirable microstructures and mechanical properties and high residual stresses and distortions, are examined in detail.

Thus, it can be stated that the additive manufacturing process using a wire arc is a very promising method for the manufacture of high-quality Ti parts. However, additional research is still required to solve the above-mentioned problems by optimizing the parameters of the process and heat treatment after deposition.

2.2. β-Ti Alloys

β-Ti alloys have excellent specific strength and fracture toughness. Among them, the Ti–5Al–5Mo–5V–3Cr alloy is most often studied for AM. This overview examines different Ti alloys produced by AM. In particular, like Ti–6Al–4V, Ti–5Al–5Mo–5V–3Cr also forms elongated grains at the boundaries of the melt bath (Figure 3a) [37]. The grains grow into a rather irregular shape with a weak <001>β-texture (Figure 3b). Unlike in Ti–6Al–4V, the Mo and Cr elements in the Ti–5Al–5Mo–5V–3Cr alloy are more prone to segregation before the solidification boundaries, which leads to the formation of a cellular–dendritic structure in the alloy after printing (Figure 3a). In addition, due to the high cooling rates during AM, a large portion of the printed Ti–5Al–5Mo–5V–3Cr alloy mainly consists of the β-phase [37]. The structure consisting of only the β-phase exhibits a good elongation at a failure of >10%, but a rather low strength of <800 MPa with an insignificant strengthening capacity [37].

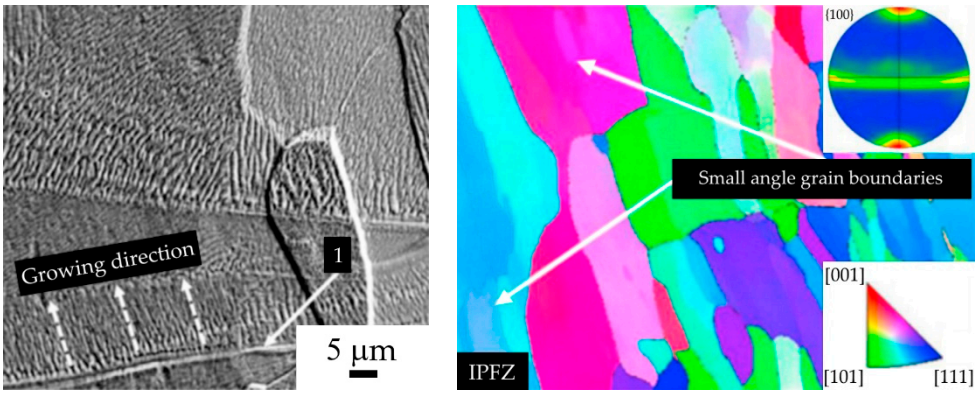

(**a**) (**b**)

Figure 3. (**a**) β grains with planar solidification mode and cellular structure. (**b**) EBSD-IPF figure showing preferred <100>β texture [37].

It is commonly believed that (β)-Ti based materials have a Young's modulus close to that of human bone. The SLM processing of the low-modulus β-Ti alloys containing non-toxic and non-allergic elements is important for the next generation of biomedical implants. An example is the alloy Ti-24Nb-4Zr-8Sn (Ti 2448), which exhibits an improved balance of a low modulus and a high strength. In their overview, the authors of [22] showed, similarly to CP Ti, that laser processing parameters must be optimized in order to produce parts with a sufficiently high density. The Vickers microhardness of the samples reached 220 HV for the almost completely dense parts (99.3%) (UTS = 665 MPa). The elastic modulus and elongation of the samples produced by SLM and conventional rolling were

closely comparable. In contrast, the tensile strength of the produced by SLM was slightly lower than for those processed by rolling or forging (830 and 755 MPa, respectively).

The overview [38] is devoted to Ti alloys of the β-type for biomedical applications. Porous Ti alloys of the β-type with a reduced elastic modulus were developed using some preparation methods, such as powder metallurgy, additive manufacturing, etc. As it was examined, Ti alloys of the β-type have comparable or even superior mechanical properties, corrosion behavior, and biocompatibility as compared to other types of Ti alloy. However, some problems with the β-type Ti alloys are noted, such as biological inertness.

Biocompatible β-Ti alloys with a high strength and low modulus are of interest for the additive manufacturing of biomedical implants. In [39], a metastable β Ti-12Mo-6Zr-2Fe (TMZF) alloy with a highly dense structure was successfully fabricated by laser powder bed fusion (LPBF) from low-cost elemental powders. The as-fabricated TMZF alloy via simple scanning strategy shows considerably high strength due to α''-, ω-phases, and sessile dislocations, but it is brittle owing to the presence of the ω-phase. The TMZF alloy, manufactured using the chess scanning strategy, possessed a high yield strength of 1026 MPa, low modulus of 85.7 GPa, and good ductility of 12.7%. This results from its unique hierarchical microstructure containing α''-phases and heterogeneous grains.

The paper [40] investigated the microstructure and mechanical properties of the SLM-produced Ti-35Nb composite (in wt%) using elemental powder. Nanoindentation revealed the presence of relatively soft undissolved Nb particles and weak interface bonding around Nb-rich regions in SLM-produced samples.

Subsequent solid solution treatment can not only improve chemical homogeneity, but also enhance bonding through grain boundary strengthening, resulting in a ∼43% increase in tensile elongation for the heat-treated Ti-35Nb compared to the SLM-produced counterpart. The SLM-produced Ti-35Nb exhibits relatively high tensile yield strength (648 ± 13 MPa) due to the formation of dendritic β grains. However, the ductility is relatively low (3.9 ± 1.1%) as a result of the weak bonding of undissolved Nb particles within the matrix. The heat-treated counterpart shows a slightly lower yield strength (602 ± 14 MPa) but a larger ductility due to the improved homogeneous Ti-Nb β phase. This provides an understanding of the homogenization of the microstructure and phases of SLM-produced alloys from an elemental powder mixture.

In [41], the addition of a small amount of boron to a β titanium alloy of the Ti-Mo system in the process of SLM led to significant changes in the microstructure. Depending on the percentage of Mo, the grain size decreased by a factor of 50–100. The change in grain size is explained by the combined action of the supercooling effect caused by the rejection of boron from growing beta grains and the grain growth limiting factor caused by dissolved alloying elements. The addition of boron also changed the grain morphology from columnar to more equiaxed. And, in the Ti-Mo system, it changes from lath to more equiaxed, while maintaining the Burgers orientation relationship between the α and β phases.

In [42], the Ti-10Mo alloys belonging to the class of beta-titanium alloys, produced by the laser deposition of powders, were studied. It was shown that the introduction of nitrogen gas during the deposition process led to the formation of the α (Ti, N) solid phase with a dendritic morphology, which was distributed in the β (TiMo) matrix. Interestingly, the addition of nitrogen, which stabilizes the α-phase in Ti, changes the solidification path and subsequent phase evolution in these alloys. Ti-Mo-N alloys have a significantly increased microhardness due to the formation of the α (Ti,N) phase, combining it with the desirable properties of the β Ti matrix, such as superior ductility, strength, and deformability. In particular, with increasing nitrogen content, the Vickers microhardness values of the Ti-Mo-N alloy increase to 800 HV compared to 500 HV for the Ti-Mo alloy deposited in pure argon.

The paper [43] reports on the production of the low-modulus β-Ti alloy, Ti–35Nb–7Zr–5Ta (TNZT), by SLM with optimized laser parameters. The final SLM-produced TNZT exhibits a high UTS (~630 MPa), excellent ductility (~15%), and a lower elastic modulus

(~81 GPa) as compared to the modern CP Ti and Ti-based alloys. The alloy's microstructure consisted of fine, equiaxed, and narrow elongated grains along the laser tracks with a mean size of 3–80 μm. The excellent mechanical strength exhibited by the SLM-produced TNZT alloy is attributed by the authors to a large quantity of local deformations as a result of rapid cooling and the high density of the dislocation network. The alloy demonstrated a low modulus perfect for biomedical applications owing to the {200} preferred orientation of the bcc crystalline structure and a large area of grain boundaries.

Thus, the method of the laser sintering of the powders of β-Ti alloys is capable of producing three-dimensional titanium alloy parts with superior mechanical properties compared to conventional methods, especially casting. However, further research is required to reduce the number of adverse factors caused by laser sintering, such as temperature gradients, residual stresses, and surface roughness.

3. Microstructure and Properties of the Ti Alloys Produced by Solid-Phase Additive Manufacturing Methods

Additive manufacturing methods based on friction welding have certain advantages over melting and solidification technologies, since the process occurs in the solid-phase state. Based on this technology, friction stir additive manufacturing, linear friction surfacing (FS), additive friction stir deposition (AFSD), and friction rolling additive manufacturing (FRAM) have been developed in recent years [9,44–49].

The schematic diagram of the layered panel formation with FSAM is shown in Figure 4. Examples of materials processed by FSAM/AFSD are Al alloys, Mg alloys, steels, and Ni-based superalloys. While the AFSD method is now easily applied to materials with a lower melting temperature, its application to high-temperature materials requires substantial research and development [44].

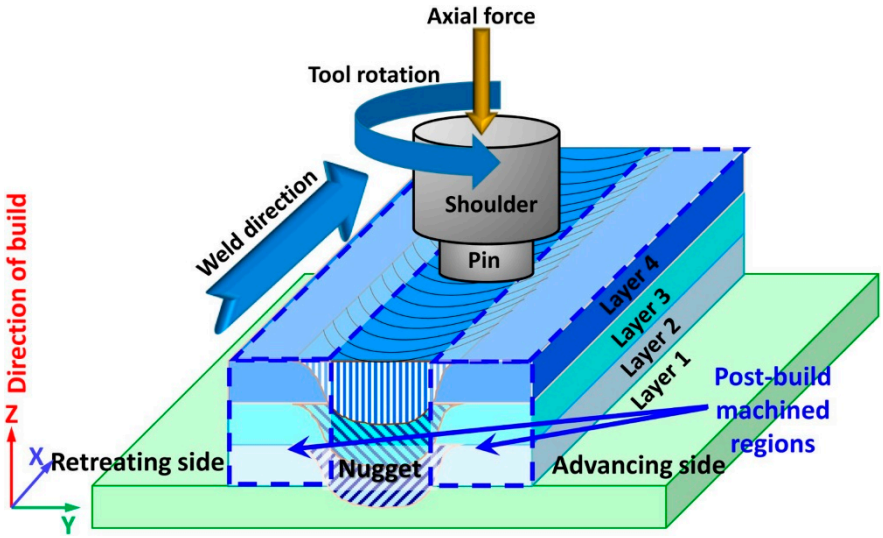

Figure 4. Schematic diagram of friction stir additive manufacturing of a stiffened panel. Four layers of build are used for this illustration, and note that the post-build machining would remove the unbonded side regions [44].

It should be noted that, over the past 5 years, the microstructure and properties of Ti-based alloys obtained by the additive FSAM method have been studied in isolated studies. In many works, researchers have studied the patterns of the formation of the macro- and microstructure of the welded joint at FSW including severe shear deformation of the material. Similar mechanisms are implemented during assembly in additive manufacturing [44].

An overview of a typical slightly enlarged cross-sectional view of a weld produced by friction stir is shown in Figure 5 [15]. Three separate zones can be easily distinguished: the

stir zone (SZ), the base material (BM), and a narrow transition region—the thermomechanically affected zone (TMAZ). The stir zone has a cup-like shape, expanding significantly towards the top. SZ is not symmetrical relative to the weld line ("kissing bond" in Figure 5), which is significantly displaced towards AS (advancing side).

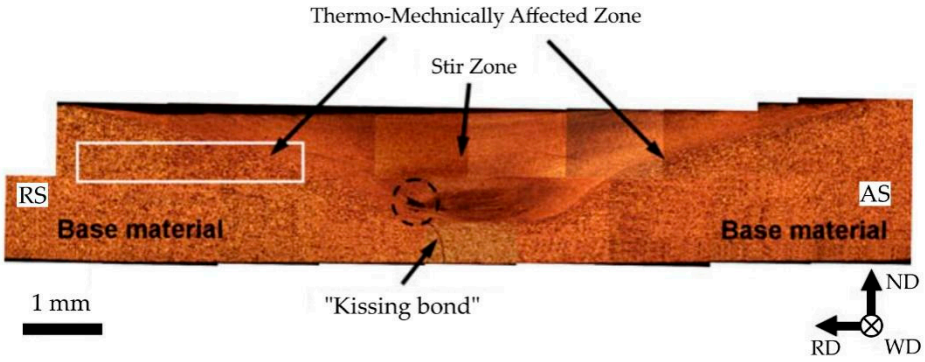

Figure 5. Low-magnification overview of the transversal cross-section of the friction stir weld. See text for details. Note: RS and AS are the retreating side and the advancing side, respectively [15].

It should be noted that titanium and its alloys belong to hexagonal close-packed (hcp) metals that usually have a limited number of independent slip systems, which has a significant impact on the evolution of the grain structure during plastic deformation.

In the first works [15], the evolution of the microstructure during the friction stir welding of CP pure titanium was studied. It was found that the material flow is close to simple shear deformation and occurs mainly due to the prismatic glide of dislocations. In this work, it was shown that the evolution of grain structure is a complex process that includes several stages. Away from the welding tool, the microstructure evolution was found to be governed by geometric deformation effects and limited intermittent recrystallization. And, in the mixing zone, the resulting texture leads to the convergence of grains, i.e., the development of grain structure is closely related to the evolution of texture.

The Ti-6Al-4V alloy is one of the most popular titanium alloys and is used in many studies. They showed that the friction stir welding (FSW) method can produce defect-free welds in the Ti-6Al-4V alloy [50–55].

The study [50] examines in detail the microstructural aspects of the formation of a weld in the titanium alloy after FSW. A typical microstructure of the Ti-6Al-4V alloy in the thickness direction of the stir zone is shown in Figure 6 [50].

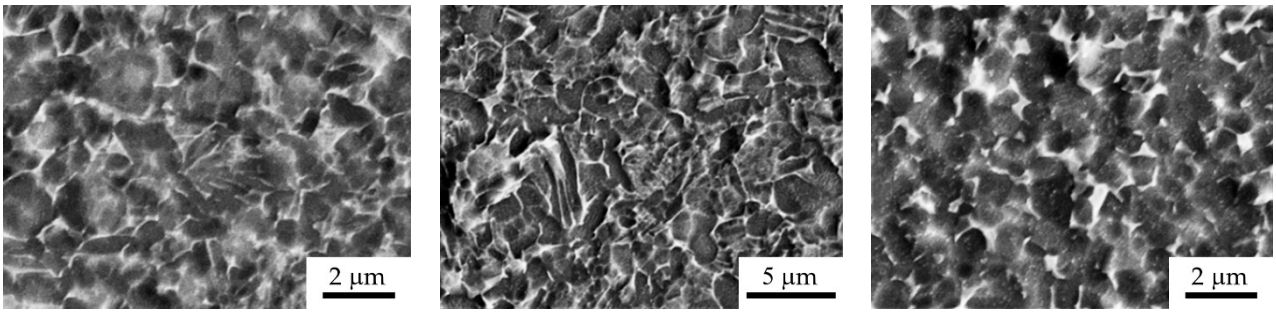

Figure 6. Typical SEM micrographs showing the microstructure distribution in the thickness direction of the stir zone: (**a**) upper section, (**b**) mid-thickness, and (**c**) bottom section. Note the difference in magnification [50].

In the SEM images of Figure 6, in all the three zones under study, a relatively small globular α-phase predominated, indicating that the processing temperature was below the

polymorphic transformation ($\alpha \rightarrow \beta$) temperature. In the upper and middle sections along the thickness of the stir zone, a significant number of secondary α-particles (α_s) were also found (Figure 6a,b). Apparently, the temperature in these areas exceeded ~900 °C and the material underwent a partial sequence of $\alpha \rightarrow \beta \rightarrow \alpha_s$ phase transformations. The finest microstructure was observed at the root of the stir zone (Figure 6b). The authors explain this fact by the relatively low conductivity temperature of titanium alloys, as well as by the fact that, during the FSW process, heating occurs as a result of friction between the workpiece surface and the tool. The coarsest microstructure was observed in the middle thickness of the stir zone (Figure 6b). Using the advanced capabilities of the EBSD method, it was shown that the microstructure formed in the stir zone is close to the microstructure after solid solution treatment at the β-transus temperature. In this case, several processes occur. In addition to the stresses causing grain refinement (common to FSW), the structure is also noticeably influenced by the partial $\alpha \rightarrow \beta \rightarrow \alpha_s$ phase transformation (caused by the thermal cycle of FSW) and interalloying due to the FSW tool wear. The non-uniform distribution of the microstructure in the stir zone indicates a significant difference in thermomechanical conditions. For example, in the microstructure formed in the central part of the stir zone, a completely globular structure of the α-phase with an average grain size of ~1 μm, the high angle boundaries fraction of 86%, and the absence of microtexture are predominant. The substructure inside individual relatively large α-grains results from the implementation of the mechanism of continuous dynamic recrystallization (CDRX) and refinement of the α-phase.

The first studies of the FSW of the Ti-6Al-4V alloy revealed a relatively narrow processing window for this method [54–57]. Many researchers believe that this is due to the relatively low ductility of Ti-6Al-4V even at elevated temperatures, as well as its low thermal conductivity, which leads to significant temperature gradients during the FSW process. Moreover, processing often lies above the polymorphic transformation (β-transus) temperature. FSW in such modes does not provide a globular microstructure, and is therefore impractical for processing two-phase materials. Another important problem is the severe wear of the processing tool [58,59]. This effect reduces tool life (thereby increasing processing costs) and leads to significant contamination of the processed material with tool impurities. Despite these disadvantages, careful control of the process parameters can achieve the desired, fully globular microstructure consisting of a fine-grained (or even ultrafine-grained) α-phase [58–64]. Regarding the microstructure of the FSW-produced alloy Ti-6Al-4V, most research has studied the influence of the welding parameters on the mechanical properties of joints. Microstructural observations have shown that the transformed β-microstructure as a result of the $\beta \rightarrow \alpha' \rightarrow \alpha$ transformation plays a key role in determining the final properties of this material [55,65,66].

In [52], welds after FSW on the Ti-6Al-4V plates were produced at different rotation speeds, and the microstructure, hardness profile, and tensile properties of the welds were studied. After FSW, a thin lamellar microstructure in the weld and a bimodal microstructure in the heat-affected zone (HAZ) were formed as a result of the solid-phase transformation and the annealing effect of the microstructure. In this case, the non-uniform distribution of the microstructure led to the anisotropy of the mechanical properties. The weld material showed much higher mechanical properties than the base material and the HAZ, which was the weakest in the weld. The UTS of the SZ was 1050 MPa compared to 920 MPa in the HAZ and base material (BM). It is obvious that the formation of a lamellar structure in the weld of titanium alloys produced by friction welding leads to a high strength compared to the base material, but also to a decrease in ductile properties (elongation 25 and 10% in the BM and SZ, respectively); therefore, during mechanical tests, the fracture of samples occurs in the base material [52].

The paper [67] is devoted to the study of the crystallographic aspects of the β-transformed structure developed in a Ti-6Al-4V alloy weld produced by friction welding. A direct comparison of the local crystallographic orientations of the α- and β-phases, as well as an analysis of the misorientation distribution of the α-phase, showed that the $\beta \rightarrow$

α phase transformation is determined by the Burgers vector. It was shown that a significant fraction of low-angle grain boundaries and the angular scatter around peak misorientation in the α-phase were attributed to the existence of a substructure in the primary β-phase before the phase transition from β to α.

The friction stir processing parameters also have a significant impact on the morphology of the weld structure. Pilchak et al. [68] investigated the effect of the friction stir processing (FSP) parameters on the microstructure of Ti-6Al-4V produced by investment casting. The authors showed that the microstructure of the SZ depends on the heat input during FSP, i.e., during FSP with a low heat input, equiaxed α-and β-grains are formed, and during FSP with a high heat input, α-/β-plates are formed. In [65], Ti-6Al-4V in the cast state was processed by FSP, after which a significant refinement of the rough, completely lamellar α-structure and, as a consequence, an increase in strength and an improved resistance to fatigue cracks were observed.

The two-phase TC4 alloy was subjected to friction stir welding using a W-Re pin tool [69]. The welded joint zone consisted of a stir zone, a heat-affected zone, and a base material. The stir zone was characterized by an equiaxed, dynamically recrystallized α-phase and a β-transformed thin lamellar α + β structure. The microstructure of the heat-affected zone is similar to the microstructure of the base material, but an increase in the volume fraction of the β-phase was observed. According to the results of tensile mechanical tests, the tensile strength of the welded joint amounted to 92% (953 and 1000 MPa, respectively) of the base material's strength. In this case, the fracture of the samples occurred in the stir zone, and the fracture surface was characterized by typical signs of plastic fracture, i.e., the stir zone is the weakest part of the joint, owing to which the tensile characteristics of the weld are preserved.

The forming microstructure in a welded joint of titanium alloys, and its anisotropy and residual stresses, has a significant impact on the mechanical behavior and propagation of fatigue cracks. This aspect was studied in [62]. The fatigue behavior of the Ti-6Al-4V alloy welded joint produced by friction stir was investigated. The authors found that, in the heat-affected zones of the weld, there was a significant evolution of the structure associated with the refinement of the α-grains, the development of a bimodal structure, and an increase in the volume fraction of the β-phase. At the same time, the residual stresses obtained using the XRD method were low, about 5% of the yield strength, in all the areas of the weld. The authors showed that, in the fine-grained zones of the welded joint (the stir zone and the interphase zone), the rate of the propagation of fatigue cracks was higher than that in the base metal and the HAZ.

In [44], the authors conducted a comprehensive study into the Ti-6Al-4V alloy produced by AFSD. The material after deposition is shown in Figure 7a. Microstructural analysis was performed on a band extracted from the plane parallel to the build direction. The sample's microstructure consisted of the α- and β-phases with a change in the β grain size from top downward, as shown in Figure 7b.

The FSAM/AFSD methods lead to the formation of a microstructure of titanium alloys similar to the structure of a welded joint during friction welding with mixing, since this can be attributed to thermomechanical processes at temperatures below the β-transus temperature. In the mixing zone using the SPO (Figure 6b) and in the friction stirrer with Ti-6Al-4V additive (Figure 7b), a typical two-phase deformed α+β structure is formed. The grain size of the β-phase and, accordingly, the length and width of the lamellae can be different depending on the type of initial structure (lamellar, equiaxed, or duplex), size, and phases, which do not greatly enlarge compared to the base material, unlike laser technologies.

As an additive manufacturing process for solids, they have the potential to eliminate several key problems associated with laser technology, in particular, undesirable porosity and residual stresses, columnar granular structure with anisotropic properties, and powder production.

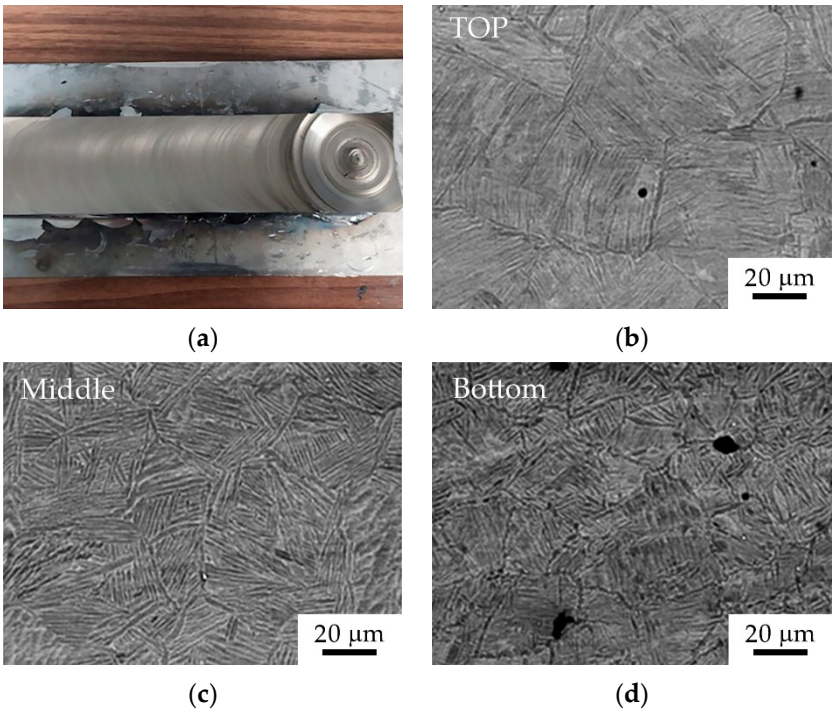

Figure 7. (**a**) Image of additive-friction-stir-deposited Ti-6Al-4V, and (**b**–**d**) backscattered images of Ti-6Al-4V from the plane parallel to the build direction [44].

4. Mechanical Properties of Titanium Alloys Obtained by Various Additive Methods

The mechanical properties of the titanium billets produced by various additive manufacturing methods are summarized for the Ti-6Al-4V alloy in Figure 8. As shown by the studies discussed above, the SLM method enables the production of bulk parts from Ti with strength properties superior to those produced, for example, by casting. This is confirmed by the data of the review [22], which reports comparative mechanical properties achieved for Ti alloys of different classes with α-, α+β, and β-structure. In this case, there is a slight decrease in ductility [68].

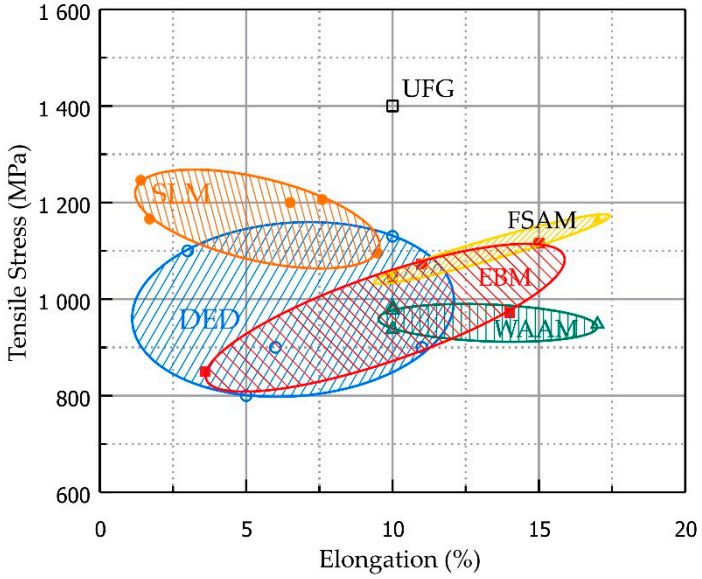

Figure 8. Mechanical properties of Ti-6Al-4V alloy synthesized by SLM, DED, EBM [22,66,69], WAAM [33], FSAM [44].

The overview [70] examines in detail the mechanical properties of the Ti-6Al-4V alloy produced by the DED and SLM processes. Peak temperatures of about 2000–2500 K and high cooling rates of about 104 K/s during the fabrication of Ti-6Al-4V result in an acicular α'-martensitic microstructure and high tensile stresses, which significantly increases the UTS and yield strength by 100–200 MPa, but reduces the ductility of the finished components. The EBM process produces a similar peak temperature range, but the high assembly temperature of 600–750 °C reduces the cooling rate locally, resulting in a residual stress-free α + β lamellar microstructure that has a similar strength and moderate ductility to the conventionally fabricated and subsequently heat-treated Ti-6Al-4V. The authors note that the α'-martensitic in the DED and SLM-produced Ti-6Al-4V structure is also responsible for lower crack thresholds but higher fatigue limits compared to the EBM-produced, deformed, forged, and heat-treated Ti-6Al-4V.

It is also reported in [19] that SLM and DED provide superior strength, which can be 25% higher than that of traditionally manufactured parts (casting, forging, rolling). However, due to the presence of higher tensile residual stress, surface roughness, and porosity, AM-produced parts have lower fatigue life and fracture toughness compared to parts produced by traditional methods.

The WAAM method for the Ti-6Al-4V alloy provides strength at a level of 1000 MPa, which is due to the large grain size of the primary β-phase with a lamellar internal structure. At the same time, the strength and ductility of the alloy depend on the process parameters. For example, in [35], it is reported that the strength can be increased to 1118 MPa by increasing the welding speed. The authors attribute this to accelerated cooling caused by narrower welds and the formation of a thinner plate structure. Increasing the wire feed speed causes the coarsening of the plates and, thus, leads to a decrease in strength.

Additive manufacturing technologies based on friction welding or friction stir welding enable the production of higher strength properties and resistance to the development of fatigue cracks [44,54,62,65,69]. For example, the UTS of some Ti-6Al-4V alloy workpieces can reach 1050 MPa, which is comparable to the UTS level of die-forged workpieces. However, the UTS of the base material and the heat-affected zone is often lower and does not exceed 920 MPa.

Thus, the considered additive manufacturing methods enable the achievement of UTS in titanium alloys comparable to forged and cast workpieces. However, due to the presence of residual stresses and porosity in laser additive technologies, the alloys have lower ductility, fatigue strength, and fracture toughness compared to traditional processing methods. FSAM methods enable the formation of a fine-grained deformed-type microstructure in titanium alloys, which contributes to a good combination of strength and ductility and, consequently, increased resistance to the development of fatigue cracks. However, systematic studies of the fatigue properties of the FSAM-produced alloy Ti-6Al-4V are currently absent.

Research over the past two decades shows that the most effective way to improve the physical and mechanical properties of commercial metals and alloys is to form ultrafine-grained structures (grain size less than 1 micron) in them using severe plastic deformation. In particular, such a “breakthrough” in achieving high physical and mechanical properties was demonstrated for light structural UFG alloys based on titanium, as indicated by many publications. For example, in the Ti-6Al-4V alloy using multiple forging, strength and endurance limits of up to 1300 and 690 MPa, respectively, were achieved, while the formation of a UFG structure with a grain size of up to 0.4 μm in the Ti-6Al-4V alloy by ECAP in combination with extrusion produced a UTS of 1450 MPa and the endurance limit reaching 700 MPa based on 10^7 cycles [71]. Such a level of mechanical properties is not yet achievable by traditional additive technologies (Figure 8). The following section presents some areas of research on ways to improve the mechanical properties of titanium alloys in additive manufacturing, including new approaches to additive manufacturing for producing ultrafine-grained titanium alloys.

5. Ways to Improve the Mechanical Properties of Titanium Alloys Produced by Additive Manufacturing

Publications over the last 10–15 years have shown that the main efforts of researchers in the field of producing titanium alloys using additive manufacturing are aimed at increasing their mechanical properties by refining the microstructure in the weld during the laser sintering of powders and wires, as well as achieving equiaxed α-structures, up to ultrafine-grained, in the additive manufacturing of titanium workpieces based on friction welding. The research directions and the achieved results are discussed in this section.

5.1. Hydrogenation of the Synthesized Material

Thermal hydrogen treatment is based on the modifying effect of hydrogen as an alloying element on the development of metastable phases and the kinetics of phase transformations in titanium alloys. In this approach, hydrogen is first added to the alloy by controlled diffusion from a hydrogen environment and then removed after the treatment.

The papers [72–74] report the use of hydrogenation to refine grains during the laser sintering of powder or wire. During the laser sintering of powder, β-columnar crystals will form in the direction of building layers in the workpiece, which leads to a decrease in the reliability of the material, causing stress concentration and the accelerated fracture of the material. In [72], the titanium alloy Ti-6Al-4V produced by the selective laser melting of powder was subjected to hydrogenation, then solid solution treatment, aging, and finally heat treatment for dehydrogenation. The research results showed that the β-grains of hydrogenated samples are refined after heat treatment. After the solid solution treatment, α'-and α''-martensites coexist in the microstructure. At the same time, since hydrogen is a β-stabilizing element, with increasing hydrogen content the β-phase becomes more stable and stabilizes at room temperature. At the same time, the amount and size of α'-and α''-martensites decrease. After aging, the original microstructure is retained, but due to the decomposition of large needle-like α''-martensite during aging, the original morphology is destroyed and a fine-grained microstructure is formed. After dehydrogenation, the fine-grained structure is retained, and the crystalline grains become equiaxed. Moreover, such a microstructure has a significant impact on the mechanical properties of the material. In particular, at room temperature, the ultimate compressive strength of hydrogenated samples after heat treatment increases and can reach 2018 MPa compared to the initial SLM state (1720 MPa).

A similar effect in the Ti-6Al-4V alloy produced by the laser sintering of powder was achieved in [73]. It was found that, with increasing hydrogen concentration, the size of large β-grains becomes smaller and finally transforms into equiaxed grains in the lower and middle parts of the samples when the hydrogen content increases to 1.0 wt%. In addition, the $\beta \rightarrow \alpha$ phase transformation temperature of the post-deposition sample decreases with increasing hydrogen content and tends to remain stable at 900 °C when the hydrogen content exceeds 0.65 wt%.

In [74], the effect of the hydrogen contents of 0.48 wt% and 1.38 wt% on the microstructure refinement of the Ti-6Al-4V alloy produced by the wire arc additive manufacturing method was investigated. In this work, the Ti-6Al-4V alloy was studied after hydrogenation, heat treatment, and dehydrogenation. It was shown that the Ti-6Al-4V alloy produced using the arc wire deposition technology consists of large columnar β-grains with a lamellar α-structure inside. After hydrogenation, the α-clusters inside the β-grains become smaller and hydrides are formed. After quenching at a temperature of T_{recr} + 10 °C, α', α'', and the metastable phase β_M were present in the microstructure. With subsequent aging and dehydrogenation, the metastable phase and hydride decomposed, which significantly refined the size of α-grains in columnar β-grains (from 5.78 μm to 0.84 μm), forming a large area of a fine-grained microstructure. It was found that, when the hydrogen content is 0.48 wt%, the morphology of α-grains after hydrogen removal is fine-needle-like, and with the hydrogen content increasing to 1.38 wt% the morphology of α-grains becomes equiaxed.

The final properties of a welded joint produced in the solid-phase state are also influenced by the initial microstructure of the material being welded. In [75], the microstructural features of the joint of Ti-6Al-4V produced by FSW at a temperature below the β-transus temperature were studied. The plates had different initial microstructures which were produced using preliminary heat treatments. Three types of initial microstructure had different densities of high-angle boundaries: an equiaxed α-structure, a coarse lamellar structure with less high-angle boundaries, and a fine α′-martensitic structure. After friction stir welding, all three states had similar characteristics: the upper surface of the SZ (Figure 9a) had a mixture of a lamellar structure with equiaxed α-grains, and the fraction of the area of equiaxed α-grains gradually increased with increasing distance from the top surface due to the temperature gradient. In this case, the average size of α-grains in a completely equiaxed region of the α-structure (Figure 9b) decreased with the increasing initial density of high-angle boundaries. The authors suggested that recrystallization is a key phenomenon in the evolution of the microstructure in the lower half where completely equiaxed grains formed, and the initial grain boundary provides a preferential location for the formation of recrystallized grains.

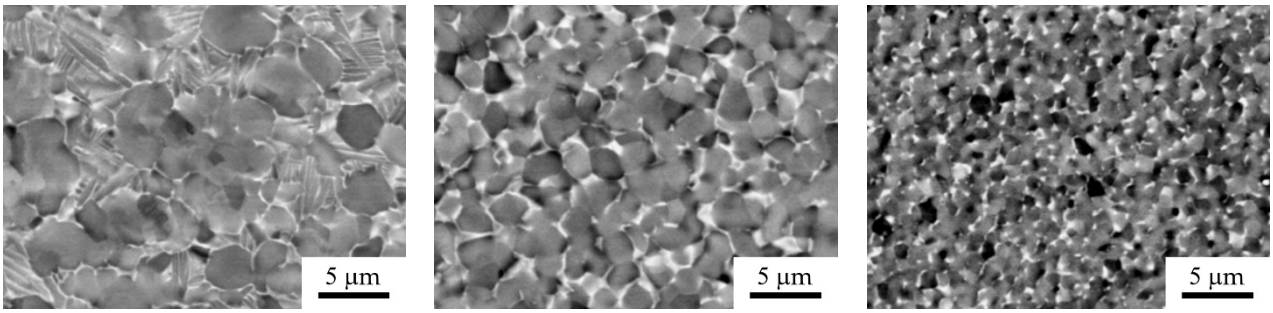

(**a**) (**b**) (**c**)

Figure 9. Microstructure of SZ obtained at as-received material joint; (**a**) top surface, (**b**) SZ center, and (**c**) bottom surface [75].

In [76], the Ti-6Al-4V alloy was subjected to thermal hydrogen treatment and friction stir welding using a W-Re pin tool. In this case, thermal hydrogen treatment improves the hot workability of titanium alloys due to increased hydrogen ductility at high temperatures. As a result of subsequent FSW and dehydrogenation treatment, a thin bimodal structure is formed, which, as known, has a higher ductility compared to lamellar structures [33].

5.2. Additional Strengthening of Synthesized Workpieces

A solution to the problem of the structure refinement of a workpiece synthesized by layer-by-layer wire deposition is proposed by combining several processes when each layer of deposited material, after cooling, is subjected to strain hardening. For example, it is shown in the papers [77–79] that the use of layer-by-layer forging in the additive manufacturing of a workpiece leads to a decrease in technological stresses, a decrease in grain size, and, as a consequence, an increase in mechanical characteristics to the level of the base metal and a decrease in the porosity and anisotropy of the metal. This approach was used during the wire plasma deposition of workpieces made of an austenitic steel of the 308LSi type in [80]. The paper [81] reports the results of a study of the additive shape forming of products made of a heat-resistant Ti-Al-V alloy using a hybrid technology of multilayer deposition CMT (Cold Metal Transfer) with layer-by-layer strain hardening (CMT Advanced), which made it possible to reduce the size of β-grains and, respectively, increase the hardness of the deposited material by about 5–7%.

In [79], a new method of laser melting deposition was used for the Ti-6Al-4V alloy to stimulate the transition from a columnar to an equiaxed structure by adding 1–5 wt% of nano-sized B_4C particles. The authors showed that the grain size decreases significantly

from 600 μm to 11 μm with increasing B_4C content. The TiB and TiC reinforcement was produced by an in situ reaction between Ti-6Al-4V and the B_4C particles, which not only precipitated at grain boundaries, limiting grain growth, but also acted as nucleation centers, accelerating the non-spontaneous nucleation of β-grains, which made it possible to achieve a fine-grained structure. Tensile tests have shown that the addition of 3 wt% of B_4C particles leads to a significant increase in yield strength (1235 MPa) and tensile strength (1310 MPa) and the retention of a certain ductility (elongation 2.4%). A similar reinforcement effect in titanium composites using a laser additive technology was observed in [82]. Thin-walled components from a titanium matrix composite reinforced with TiC + TiB were manufactured in situ by mixing the Ti-6Al-4V alloy powder and B_4C particles using the laser melting deposition technology. In [83], selective laser melting was also used to produce samples of the TiC/($TiAl_3$ + Ti_3AlC_2) composite. Despite the partial growth of grains during the preparation process, the microstructure was refined, and the size of the reinforced phases did not exceed 1 μm.

In [84], an in situ design approach to create spatially modulated alloys using laser powder melting is demonstrated. It is shown that the partial homogenization of two dissimilar alloys, Ti-6Al-4V and a small amount of the 316L stainless steel, enables the production of the micrometer-scale concentration modulations of the elements contained in 316L in the Ti-6Al-4V matrix. The corresponding modulation of phase stability creates a small-scale modulated β + α′ two-phase microstructure that exhibits a positive transformation-induced plasticity effect, resulting in a high tensile strength of ~1.3 GPa with a uniform elongation of ~9% and an excellent strengthening capacity of >300 MPa. This approach paves the way for concentration-modulated dissimilar alloy design for structural and functional applications.

Thus, the increased properties of titanium workpieces produced by the additive technologies of the selective laser melting of powder or wire can be achieved by refining the microstructure through thermal hydrogen treatment after the synthesis of the workpiece by using strain hardening between layers, by introducing the reinforcing additives of nano-sized particles of a high hardness, and by the in situ design of a material from dissimilar alloys. The effectiveness of thermal hydrogen treatment for the formation of equiaxed grains in the microstructure of workpieces produced by an additive technology based on friction welding has been confirmed.

5.3. Prospects for Producing Nanostructured Titanium Alloys: New Challenges

As is known, the strength properties of titanium alloys depend on the morphology of the α-phase and the sizes of β-grains, which are varied by the temperature and heating rate of the material, as well as the cooling rate [33]. At the same time, it has been proven [16] that reducing the grain size in metals to values in the range of 0.1–1.0 μm using SPD processing leads to the significant strengthening of the material due to an increase in the length of grain boundaries and an increase in dislocation density, i.e., the involvement of the grain boundary and dislocation strengthening mechanisms. The formation of nanostructured and UFG states by SPD processing in the α, α + β, and β class titanium alloys made it possible to achieve a high strength and endurance limit, almost 20–50% higher than for alloys produced by commercial methods (forging, die forging, rolling, etc.). In particular, using the methods of equal channel angular pressing (ECAP) and ECAP-Conform (ECAP-C), a unique combination of strength and ductility was produced in the CP Ti Grade 4 alloy, Ti-6Al-4V [71], and Ti-15Mo [85–88]. It can be assumed that the use of nanostructured rods and wires in the synthesis of workpieces using additive manufacturing will make it possible to produce parts with an even smaller grain size and higher strength properties.

In the study [89], a solution to the problem of increasing the strength properties of the Ti-6Al-4V alloy synthesized by additive wire deposition welding is proposed through the use of a wire with an initial UFG structure produced by ECAP in combination with drawing. This work shows that, in the microstructure of the sample produced using a UFG wire, the fraction of the α-phase reaches 93%, as compared to the equilibrium composition where its fraction is approximately 85% [32]. The average microhardness values of the

metal deposited using a wire with a UFG structure are approximately 20% higher than the microhardness of the sample grown using a conventional welding wire. Both factors, such as the smaller thickness of the lamellae and a higher proportion of the "solid" α-phase, led to the increased microhardness of the material grown with a UFG wire compared to the sample produced with a standard wire (410 ± 15 and 360 ± 20 HV, respectively) (Figure 10).

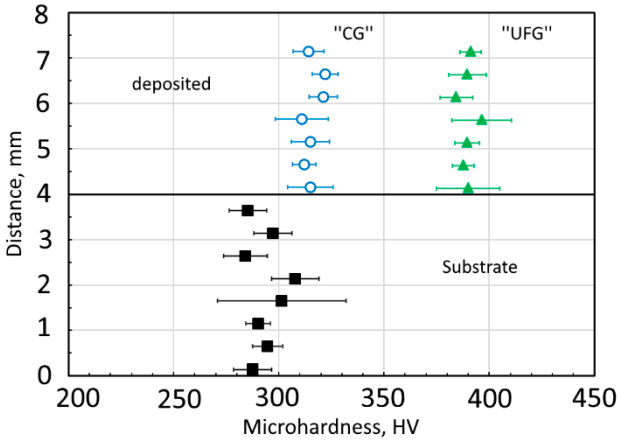

Figure 10. Microhardness in the section of the Ti-6Al-4V alloy samples produced using standard CG and UFG wires [89].

The authors explain this phenomenon by the presence in the melt of non-equilibrium groups characterized by a "short-range order" inherited from the source material. Apparently, such clusters and non-equilibrium atomic groups can serve as nucleation centers for the α-phase during the subsequent cooling of the deposited layer. In this case, an increase in such centers leads to the formation of thinner and shorter α-phase lamellae (Figure 11).

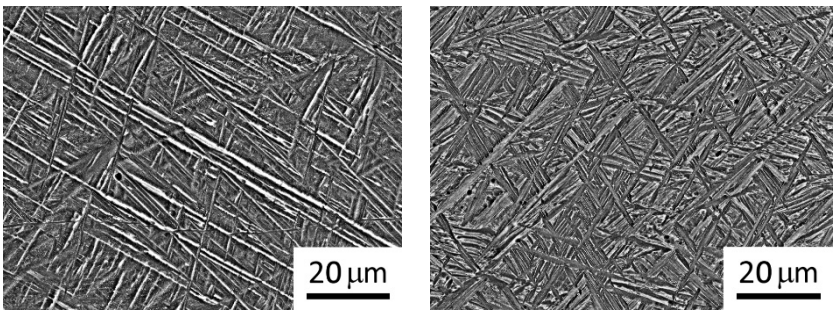

(**a**) (**b**)

Figure 11. SEM images of the intragranular microstructure of the samples produced by layer-by-layer deposition welding in three cycles using a wire with a conventional structure (**a**) and UFG structure (**b**) [89].

The initial microstructure of the material will have a significant impact on the properties of the welded joint produced by an additive technology based on friction welding. When friction welding occurs in the contact zone of rubbing surfaces, heating occurs at a rate of thousands of degrees per second. Therefore, in combination with a high rate and intensity of shear deformation against the background of a compressive load, a decrease in grain size and the formation of a UFG or nanocrystalline structure in the weld itself occur. This creates the prerequisites for the occurrence of the effect of low-temperature superplasticity, which has been discovered in many nanostructured materials [16,90]. According to modern concepts, superplasticity is realized by the action of cooperative shear bands, with the predominant participation of grain boundary sliding [16].

For example, the work [91] shows the role of high-strain-rate superplasticity in the formation of a welded joint during the linear friction welding of two-phase titanium alloys, including those with a previously prepared UFG structure. The main differences in the mechanisms of the formation of a welded joint of titanium alloys in the fine-grained (FG–about 5 μm) and UFG (0.6 μm) states were demonstrated. In the case of the VT8-1/VT6 pair in the FG states, the microstructure of the weld zone consisted of micro-needle-like martensite, characteristic of the rapid cooling of the alloy from the β-region. In the UFG version of the initial workpiece, the microstructure of the central layer of the weld was characterized by martensitic plates in the nanoscale range (thickness 30. . .75 nm), almost indistinguishable at the same magnification as the FG joint.

During the friction welding of alloys in the UFG state, apparently, the same mechanism of microstructure transformation is realized as in the case of the FG state; but, due to the higher deformability of the UFG material, the zone of intense deformation becomes wider compared to the FG version. As a result, the hot zone becomes less localized and the maximum temperature is lower. The alloy retains the two-phase state which is most favorable for the implementation of high-strain-rate superplasticity. The structure of the welded joint, in this case, is distinguished by the presence of a residual α-phase in the weld, a smaller and more uniform structure, a blurred boundary between the weld and the TMAZ, and a smooth change in microhardness along the cross-section of the welded joint (Figure 12). All this has a positive effect on the properties of the joint: the strength corresponds to the base material, both under static and cyclic loading.

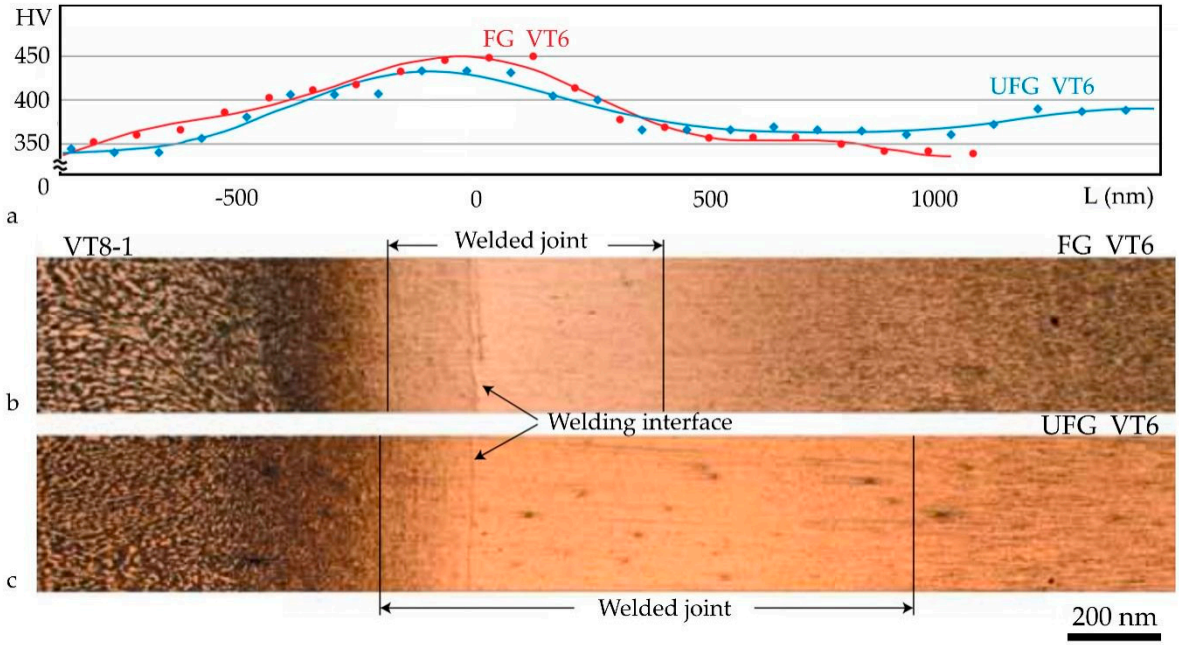

Figure 12. Microhardness (**a**) and microstructure (**b**,**c**) of the joint of VT8-1 with VT6 [91].

The mechanisms described above determine the structural features of the welded joints of titanium alloys produced by additive manufacturing in the solid-phase state. Moreover, in the case of transition to materials in a submicroscopic or UFG state, the role of high-strain-rate superplasticity will increase. On the one hand, high-strain-rate superplasticity ensures the extrusion of contaminants present on the surfaces being welded into a burr, the absence of overheating in the welding zone, and a high degree of deformation necessary to create physical contact and form a welded joint.

Thus, the application of additive manufacturing for the production of parts and products from Ti alloys with an ultrafine-grained structure is a new direction of research. This opens up the possibility of producing structural elements of complex configurations from titanium alloys with ultrafine grain sizes and, therefore, with high performance

properties, in demand in such high-tech industries as aircraft building, ship building, chemical engineering, and power engineering.

One of the promising approaches proposed by the authors of this overview is the use of the friction stir welding method and rods and bars made of titanium alloys with a UFG structure produced by SPD processing. In this case, the result of microstructure refinement in the synthesized workpieces can be achieved not only through the use of the FSW method itself (due to friction with stirring implemented with the achievement of large degrees of deformation), but also through a preliminary microstructure refinement of the material using SPD processing. In addition, in the process of the FSW of rods with a UFG structure, the role of the superplasticity of the material increases, which is realized under conditions of elevated temperatures in the contact zone, which will enable an increase in the rate of layer-by-layer deposition and the quality of the microstructure and properties. The use of thermal hydrogen treatment will improve the deformability of titanium alloys, both at the stage of the nanostructuring of workpieces using the SPD method and at the stage of producing bulk workpieces using the FSW method. In this case, the implementation of the synergistic effect from the nanostructuring of initial materials in combination with additive technologies and finishing thermal hydrogen treatment opens up new opportunities for producing high-strength products from nanostructured titanium materials.

6. Summary

1. Research in the area of additive manufacturing, as applied to Ti alloys with α, α + β, and β structures, is developing at a great pace, and the obtained results open up prospects for their application in the manufacturing of products and semi-products that are in demand in the aerospace, biomedical, and oil and gas industries.

2. The use of laser technologies with powder or wire, when the successive melting and solidification of the alloy occurs, forms a coarse-grained dendritic structure, which often does not provide the strength and fatigue properties of alloys achieved by traditional methods, such as rolling, forging, die-forging, etc. The main efforts of researchers are aimed at reducing such unfavorable factors as increased porosity, residual stresses, and surface roughness.

3. To achieve a fine-grained structure in titanium workpieces synthesized by laser methods, various methods and approaches are used, such as thermal hydrogen treatment, additional hardening between processing cycles, the introduction of hardening particles, the in situ fusion of dissimilar metal powders, etc.

4. Additional technologies in the solid-phase state of titanium alloys are attracting ever increasing attention, since the temperature of local heating in the contact zone of the material with the tool can be lower than the temperature of the polymorphic transformation. On the one hand, this contributes to the formation of a fine grain in the stir zone; on the other hand, this allows you to keep the grain size of the base material, thereby increasing the strength of the synthesized material.

5. The use of friction stir additive manufacturing technologies to form an ultrafine-grained structure in complex-shaped parts requires an integrated approach to processing which includes the preliminary preparation of the ultrafine structure in the initial rods/bars using thermal hydrogen treatment and severe plastic deformation. The use of such an integrated approach for titanium alloys of α, α + β, and β class requires solving both material science and technological problems, which will be the focus of the efforts of the team of authors of this overview in the near future.

Author Contributions: Conceptualization, I.V.A., Z.S. and I.P.S.; methodology, A.V.P.; validation, I.V.A., Z.S. and Y.D.; writing—original draft preparation, I.P.S. and A.V.P.; writing—review and editing, A.V.P. and Y.D.; supervision, I.V.A.; project administration, I.V.A. and Z.S.; funding acquisition, I.V.A. All authors have read and agreed to the published version of the manuscript.

Funding: This research was funded by the Russian Science Foundation, grant No. 23-43-00041 (https://rscf.ru/project/23-43-00041/ accessed on 21 August 2024), and the National Natural Science Foundation of China, grant No. 52261135539.

Data Availability Statement: The data presented in this study are available on request from the corresponding author.

Conflicts of Interest: The authors declare no conflicts of interest.

References

1. Veiga, C.; Davim, J.; Loureiro, A. Properties and Applications of Titanium Alloys: A Brief Review. *Rev. Adv. Mater. Sci.* **2012**, *32*, 133–148.
2. Zhao, Q.; Sun, Q.; Xin, S.; Chen, Y.; Wu, C.; Wang, H.; Xu, J.; Wan, M.; Zeng, W.; Zhao, Y. High-Strength Titanium Alloys for Aerospace Engineering Applications: A Review on Melting-Forging Process. *Mater. Sci. Eng. A* **2022**, *845*, 143260. [CrossRef]
3. Liu, Z.; He, B.; Lyu, T.; Zou, Y. A Review on Additive Manufacturing of Titanium Alloys for Aerospace Applications: Directed Energy Deposition and Beyond Ti-6Al-4V. *JOM* **2021**, *73*, 1804–1818. [CrossRef]
4. Shahrubudin, N.; Lee, T.C.; Ramlan, R. An Overview on 3D Printing Technology: Technological, Materials, and Applications. *Procedia Manuf.* **2019**, *35*, 1286–1296. [CrossRef]
5. Barriobero-Vila, P.; Gussone, J.; Stark, A.; Schell, N.; Haubrich, J.; Requena, G. Peritectic Titanium Alloys for 3D Printing. *Nat. Commun.* **2018**, *9*, 3426. [CrossRef] [PubMed]
6. DebRoy, T.; Wei, H.L.; Zuback, J.S.; Mukherjee, T.; Elmer, J.W.; Milewski, J.O.; Beese, A.M.; Wilson-Heid, A.; De, A.; Zhang, W. Additive Manufacturing of Metallic Components–Process, Structure and Properties. *Prog. Mater. Sci.* **2018**, *92*, 112–224. [CrossRef]
7. Ding, D.; Pan, Z.; Cuiuri, D.; Li, H. Wire-Feed Additive Manufacturing of Metal Components: Technologies, Developments and Future Interests. *Int. J. Adv. Manuf. Technol.* **2015**, *81*, 465–481. [CrossRef]
8. Wu, B.; Pan, Z.; Ding, D.; Cuiuri, D.; Li, H.; Xu, J.; Norrish, J. A Review of the Wire Arc Additive Manufacturing of Metals: Properties, Defects and Quality Improvement. *J. Manuf. Process.* **2018**, *35*, 127–139. [CrossRef]
9. Dilip, J.J.S.; Ram, G.D.J.; Stucker, B.E. Additive Manufacturing with Friction Welding and Friction Deposition Processes. *Int. J. Rapid Manuf.* **2012**, *3*, 56–69. [CrossRef]
10. Dilip, J.J.S.; Babu, S.; Rajan, S.V.; Rafi, K.H.; Ram, G.D.J.; Stucker, B.E. Use of Friction Surfacing for Additive Manufacturing. *Mater. Manuf. Process.* **2013**, *28*, 189–194. [CrossRef]
11. Enomoto, M. Friction Stir Welding: Research and Industrial Applications. *Weld. Int.* **2003**, *17*, 341–345. [CrossRef]
12. Okamura, H.; Aota, K.; Takai, H.; Ezumi, M. Problems for Application and Situation of Development in Friction Stir Welding. *J. Jpn. Weld. Soc.* **2003**, *72*, 436–444. [CrossRef]
13. Mishra, R.S.; Ma, Z.Y. Friction Stir Welding and Processing. *Mater. Sci. Eng. R Rep.* **2005**, *50*, 1–78. [CrossRef]
14. Park, S.H.C.; Sato, Y.S.; Kokawa, H.; Okamoto, K.; Hirano, S.; Inagaki, M. Microstructural Characterisation of Stir Zone Containing Residual Ferrite in Friction Stir Welded 304 Austenitic Stainless Steel. *Sci. Technol. Weld. Join.* **2005**, *10*, 550–556. [CrossRef]
15. Mironov, S.; Sato, Y.S.; Kokawa, H. Development of Grain Structure during Friction Stir Welding of Pure Titanium. *Acta Mater.* **2009**, *57*, 4519–4528. [CrossRef]
16. Valiev, R.Z.; Zhilyaev, A.P.; Langdon, T.G. *Bulk Nanostructured Materials: Fundamentals and Applications*, 1st ed.; Wiley: Hoboken, NJ, USA, 2013; ISBN 978-1-118-09540-9.
17. Kiran, M.B. Additive Manufacturing of Titanium Alloys—A Review. In Proceedings of the International Conference on Industrial Engineering and Operations Management, Singapore, 7–11 March 2021; IEOM Society International: Singapore.
18. Leon, A.; Levy, G.K.; Ron, T.; Shirizly, A.; Aghion, E. The Effect of Hot Isostatic Pressure on the Corrosion Performance of Ti-6Al-4 V Produced by an Electron-Beam Melting Additive Manufacturing Process. *Addit. Manuf.* **2020**, *33*, 101039. [CrossRef]
19. Nguyen, H.D.; Pramanik, A.; Basak, A.K.; Dong, Y.; Prakash, C.; Debnath, S.; Shankar, S.; Jawahir, I.S.; Dixit, S.; Buddhi, D. A Critical Review on Additive Manufacturing of Ti-6Al-4V Alloy: Microstructure and Mechanical Properties. *J. Mater. Res. Technol.* **2022**, *18*, 4641–4661. [CrossRef]
20. Zhang, X.; Liu, S.; Liu, Y.; Guo, H.; Shi, W. Titanium Alloy Fabricated by Additive Manufacturing for Medical Applications: Obtaining, Characterization and Application—Review. *Metals* **2023**, *13*, 462. [CrossRef]
21. Cao, S.; Zou, Y.; Lim, C.V.S.; Wu, X. Review of Laser Powder Bed Fusion (LPBF) Fabricated Ti-6Al-4V: Process, Post-Process Treatment, Microstructure, and Property. *Light Adv. Manuf.* **2021**, *2*, 313–332. [CrossRef]
22. Zhang, L.-C.; Attar, H.; Calin, M.; Eckert, J. Review on Manufacture by Selective Laser Melting and Properties of Titanium Based Materials for Biomedical Applications. *Mater. Technol.* **2016**, *31*, 66–76. [CrossRef]
23. Hao, Y.-L.; Li, S.-J.; Yang, R. Biomedical Titanium Alloys and Their Additive Manufacturing. *Rare Met.* **2016**, *35*, 661–671. [CrossRef]
24. Hemes, S.; Meiners, F.; Sizova, I.; Hama-Saleh, R.; Röhrens, D.; Weisheit, A.; Häfner, C.; Bambach, M. Microstructures and Mechanical Properties of Hybrid, Additively Manufactured Ti6Al4V after Thermomechanical Processing. *Materials* **2021**, *14*, 1039. [CrossRef] [PubMed]
25. Eskandari Sabzi, H. Powder Bed Fusion Additive Layer Manufacturing of Titanium Alloys. *Mater. Sci. Technol.* **2019**, *35*, 875–890. [CrossRef]

26. Treutler, K.; Wesling, V. The Current State of Research of Wire Arc Additive Manufacturing (WAAM): A Review. *Appl. Sci.* **2021**, *11*, 8619. [CrossRef]
27. Long, P.; Wen, D.; Min, J.; Zheng, Z.; Li, J.; Liu, Y. Microstructure Evolution and Mechanical Properties of a Wire-Arc Additive Manufactured Austenitic Stainless Steel: Effect of Processing Parameter. *Materials* **2021**, *14*, 1681. [CrossRef]
28. Brandl, E.; Schoberth, A.; Leyens, C. Morphology, Microstructure, and Hardness of Titanium (Ti-6Al-4V) Blocks Deposited by Wire-Feed Additive Layer Manufacturing (ALM). *Mater. Sci. Eng. A* **2012**, *532*, 295–307. [CrossRef]
29. Haghdadi, N.; Laleh, M.; Moyle, M.; Primig, S. Additive Manufacturing of Steels: A Review of Achievements and Challenges. *J. Mater. Sci.* **2021**, *56*, 64–107. [CrossRef]
30. Mok, S.H.; Bi, G.; Folkes, J.; Pashby, I.; Segal, J. Deposition of Ti–6Al–4V Using a High Power Diode Laser and Wire, Part II: Investigation on the Mechanical Properties. *Surf. Coat. Technol.* **2008**, *202*, 4613–4619. [CrossRef]
31. Syed, A.K.; Zhang, X.; Caballero, A.; Shamir, M.; Williams, S. Influence of Deposition Strategies on Tensile and Fatigue Properties in a Wire + Arc Additive Manufactured Ti-6Al-4V. *Int. J. Fatigue* **2021**, *149*, 106268. [CrossRef]
32. Welsch, G.; Boyer, R.; Collings, E.W. (Eds.) *Materials Properties Handbook: Titanium Alloys*; ASM International: Materials Park, OH, USA, 1994; ISBN 978-0-87170-481-8.
33. Lütjering, G.; Williams, J.C. *Titanium*, 2nd ed.; Engineering Materials and Processes; Springer: Berlin/Heidelberg, Germany, 2007; ISBN 978-3-540-71397-5.
34. Bergmann, J.P. Laserstrahlschweißen von Titanwerkstoffen Unter Berücksichtigung Des Einflusses Des Sauerstoffes. *Mater. Werkst.* **2004**, *35*, 543–556. [CrossRef]
35. Elitzer, D.; Höppel, H.W.; Göken, M.; Baier, D.; Fuchs, C.; Bähr, H.; Meyer, T.; Gallasch, A. Influence of Wire Arc Additive Manufacturing of Ti-6Al-4V on Microstructure and Mechanical Properties for Potential Large-Scale Aviation Parts. *MATEC Web Conf.* **2020**, *321*, 03037. [CrossRef]
36. Raut, L.P.; Taiwade, R.V. Wire Arc Additive Manufacturing: A Comprehensive Review and Research Directions. *J. Mater. Eng. Perform.* **2021**, *30*, 4768–4791. [CrossRef]
37. Zhang, T.; Liu, C.-T. Design of Titanium Alloys by Additive Manufacturing: A Critical Review. *Adv. Powder Mater.* **2022**, *1*, 100014. [CrossRef]
38. Chen, L.-Y.; Cui, Y.-W.; Zhang, L.-C. Recent Development in Beta Titanium Alloys for Biomedical Applications. *Metals* **2020**, *10*, 1139. [CrossRef]
39. Duan, R.; Li, S.; Cai, B.; Zhu, W.; Ren, F.; Attallah, M.M. A High Strength and Low Modulus Metastable β Ti-12Mo-6Zr-2Fe Alloy Fabricated by Laser Powder Bed Fusion in-Situ Alloying. *Addit. Manuf.* **2021**, *37*, 101708. [CrossRef]
40. Wang, J.; Liu, Y.; Rabadia, C.D.; Liang, S.-X.; Sercombe, T.B.; Zhang, L.-C. Microstructural Homogeneity and Mechanical Behavior of a Selective Laser Melted Ti-35Nb Alloy Produced from an Elemental Powder Mixture. *J. Mater. Sci. Technol.* **2021**, *61*, 221–233. [CrossRef]
41. Mantri, S.A.; Alam, T.; Choudhuri, D.; Yannetta, C.J.; Mikler, C.V.; Collins, P.C.; Banerjee, R. The Effect of Boron on the Grain Size and Texture in Additively Manufactured β-Ti Alloys. *J. Mater. Sci.* **2017**, *52*, 12455–12466. [CrossRef]
42. Borkar, T.; Gopagoni, S.; Nag, S.; Hwang, J.Y.; Collins, P.C.; Banerjee, R. In Situ Nitridation of Titanium–Molybdenum Alloys during Laser Deposition. *J. Mater. Sci.* **2012**, *47*, 7157–7166. [CrossRef]
43. Ummethala, R.; Karamched, P.S.; Rathinavelu, S.; Singh, N.; Aggarwal, A.; Sun, K.; Ivanov, E.; Kollo, L.; Okulov, I.; Eckert, J.; et al. Selective Laser Melting of High-Strength, Low-Modulus Ti–35Nb–7Zr–5Ta Alloy. *Materialia* **2020**, *14*, 100941. [CrossRef]
44. Mishra, R.S.; Haridas, R.S.; Agrawal, P. Friction Stir-Based Additive Manufacturing. *Sci. Technol. Weld. Join.* **2022**, *27*, 141–165. [CrossRef]
45. Kim, J.-D.; Peng, Y. Plunging Method for Nd:YAG Laser Cladding with Wire Feeding. *Opt. Lasers Eng.* **2000**, *33*, 299–309. [CrossRef]
46. Kim, J.D.; Kang, K.H.; Kim, J.N. Nd: YAG Laser Cladding of Marine Propeller with Hastelloy C-22. *Appl. Phys. A* **2004**, *79*, 1583–1585. [CrossRef]
47. Gopan, V.; Leo Dev Wins, K.; Surendran, A. Innovative Potential of Additive Friction Stir Deposition among Current Laser Based Metal Additive Manufacturing Processes: A Review. *CIRP J. Manuf. Sci. Technol.* **2021**, *32*, 228–248. [CrossRef]
48. Hassan, A.; Pedapati, S.R.; Awang, M.; Soomro, I.A. A Comprehensive Review of Friction Stir Additive Manufacturing (FSAM) of Non-Ferrous Alloys. *Materials* **2023**, *16*, 2723. [CrossRef] [PubMed]
49. Pattanashetti, N. Recent Advances in Friction Stir Additive Manufacturing: A Comprehensive Review. *Int. J. All Res. Educ. Sci. Methods* **2024**, *12*, 2645–2648.
50. Mironov, S.; Sato, Y.S.; Kokawa, H.; Hirano, S.; Pilchak, A.L.; Semiatin, S.L. Microstructural Characterization of Friction-Stir Processed Ti-6Al-4V. *Metals* **2020**, *10*, 976. [CrossRef]
51. Lienert, T.J. Microstucture and Mechanical Properties of Friction Stir Welded Titanium alloys. In *Friction Stir Welding and Processing*; Mishra, R.S., Mahoney, M.W., Eds.; ASM International: Materials Park, OH, USA, 2007; pp. 123–155. ISBN 978-0-87170-848-9.
52. Zhang, Y.; Sato, Y.S.; Kokawa, H.; Park, S.H.C.; Hirano, S. Microstructural Characteristics and Mechanical Properties of Ti–6Al–4V Friction Stir Welds. *Mater. Sci. Eng. A* **2008**, *485*, 448–455. [CrossRef]
53. Mironov, S. Microstructural Aspects of Friction Stir Welding. *IOP Conf. Ser. Mater. Sci. Eng.* **2021**, *1014*, 012024. [CrossRef]
54. Lauro, A. Friction Stir Welding of Titanium Alloys. *Weld. Int.* **2012**, *26*, 8–21. [CrossRef]

55. Su, J.; Wang, J.; Mishra, R.S.; Xu, R.; Baumann, J.A. Microstructure and Mechanical Properties of a Friction Stir Processed Ti–6Al–4V Alloy. *Mater. Sci. Eng. A* **2013**, *573*, 67–74. [CrossRef]
56. Edwards, P.D.; Ramulu, M. Investigation of Microstructure, Surface and Subsurface Characteristics in Titanium Alloy Friction Stir Welds of Varied Thicknesses. *Sci. Technol. Weld. Join.* **2009**, *14*, 476–483. [CrossRef]
57. Edwards, P.D.; Ramulu, M. Comparative Study of Fatigue and Fracture in Friction Stir and Electron Beam Welds of 24 Mm Thick Titanium Alloy Ti-6Al-4 V. *Fatigue Fract. Eng. Mater. Struct.* **2016**, *39*, 1226–1240. [CrossRef]
58. Pilchak, A.L.; Juhas, M.C.; Williams, J.C. Observations of Tool-Workpiece Interactions during Friction Stir Processing of Ti-6Al-4V. *Met. Mater. Trans. A* **2007**, *38*, 435–437. [CrossRef]
59. Wang, J.; Su, J.; Mishra, R.S.; Xu, R.; Baumann, J.A. Tool Wear Mechanisms in Friction Stir Welding of Ti–6Al–4V Alloy. *Wear* **2014**, *321*, 25–32. [CrossRef]
60. Pilchak, A.L.; Norfleet, D.M.; Juhas, M.C.; Williams, J.C. Friction Stir Processing of Investment-Cast Ti-6Al-4V: Microstructure and Properties. *Met. Mater. Trans. A* **2008**, *39*, 1519–1524. [CrossRef]
61. Pilchak, A.L.; Juhas, M.C.; Williams, J.C. Microstructural Changes Due to Friction Stir Processing of Investment-Cast Ti-6Al-4V. *Met. Mater. Trans. A* **2007**, *38*, 401–408. [CrossRef]
62. Muzvidziwa, M.; Okazaki, M.; Suzuki, K.; Hirano, S. Role of Microstructure on the Fatigue Crack Propagation Behavior of a Friction Stir Welded Ti–6Al–4V. *Mater. Sci. Eng. A* **2016**, *652*, 59–68. [CrossRef]
63. Yoon, S.; Ueji, R.; Fujii, H. Microstructure and Texture Distribution of Ti–6Al–4V Alloy Joints Friction Stir Welded below β-Transus Temperature. *J. Mater. Process. Technol.* **2016**, *229*, 390–397. [CrossRef]
64. Ma, Z.Y.; Pilchak, A.L.; Juhas, M.C.; Williams, J.C. Microstructural Refinement and Property Enhancement of Cast Light Alloys via Friction Stir Processing. *Scr. Mater.* **2008**, *58*, 361–366. [CrossRef]
65. Ramirez, A.J.; Juhas, M.C. Microstructural Evolution in Ti-6Al-4V Friction Stir Welds. *Mater. Sci. Forum* **2003**, *426–432*, 2999–3004. [CrossRef]
66. John, R.; Jata, K.; Sadananda, K. Residual Stress Effects on Near-Threshold Fatigue Crack Growth in Friction Stir Welds in Aerospace Alloys. *Int. J. Fatigue* **2003**, *25*, 939–948. [CrossRef]
67. Mironov, S.; Zhang, Y.; Sato, Y.S.; Kokawa, H. Crystallography of Transformed β Microstructure in Friction Stir Welded Ti–6Al–4V Alloy. *Scr. Mater.* **2008**, *59*, 511–514. [CrossRef]
68. Pilchak, A.L. The Relationship between Friction Stir Process (FSP) Parameters and Microstructure in Investment Cast TI-6AL-4V. In *Friction Stir Welding and Processing*; TMS: Warrendale, PA, USA, 2007; Volume IV, pp. 419–428.
69. Liu, H.; Zhou, L. Microstructural Zones and Tensile Characteristics of Friction Stir Welded Joint of TC4 Titanium Alloy. *Trans. Nonferrous Met. Soc. China* **2010**, *20*, 1873–1878. [CrossRef]
70. Liu, S.; Shin, Y.C. Additive Manufacturing of Ti6Al4V Alloy: A Review. *Mater. Des.* **2019**, *164*, 107552. [CrossRef]
71. Semenova, I.P.; Polyakova, V.V.; Dyakonov, G.S.; Polyakov, A.V. Ultrafine-Grained Titanium-Based Alloys: Structure and Service Properties for Engineering Applications. *Adv. Eng. Mater.* **2020**, *22*, 1900651. [CrossRef]
72. Guo, Y.; Fang, Y.; Dai, G.; Sun, Z.; Wang, Y.; Yuan, Q. The Effect of Hydrogen Treatment on Microstructures Evolution and Mechanical Properties of Titanium Alloy Fabricated by Selective Laser Melting. *J. Alloys Compd.* **2022**, *890*, 161642. [CrossRef]
73. Sun, Z.; Qi, F.; Guo, Y.; Wang, Y.; Chang, H.; Wu, F.; Chen, W.; Ji, X. The Effect of Hydrogen on the Grain Refinement and Mechanisms for Ti6Al4V Alloys during Laser Melting Deposition. *J. Alloys Compd.* **2021**, *877*, 160122. [CrossRef]
74. Xiaolong, C.; Zulei, L.; Yanhua, G.; Zhonggang, S.; Yaoqi, W.; Lian, Z. A Study on the Grain Refinement Mechanism of Ti-6Al-4V Alloy Produced by Wire Arc Additive Manufacturing Using Hydrogenation Treatment Processes. *J. Alloys Compd.* **2022**, *890*, 161634. [CrossRef]
75. Yoon, S.; Ueji, R.; Fujii, H. Effect of Initial Microstructure on Ti–6Al–4V Joint by Friction Stir Welding. *Mater. Des.* **2015**, *88*, 1269–1276. [CrossRef]
76. Liu, H.J.; Zhou, L.; Liu, Q.W. Microstructural Evolution Mechanism of Hydrogenated Ti–6Al–4V in the Friction Stir Welding and Post-Weld Dehydrogenation Process. *Scr. Mater.* **2009**, *61*, 1008–1011. [CrossRef]
77. Martina, F.; Williams, S.W.; Colegrove, P.A. Improved Microstructure and Increased Mechanical Properties of Additive Manufacture Produced Ti–6Al–4V by Interpass Cold Rolling. In Proceedings of the 24th International Solid Freeform Fabrication Symposium, Austin, TX, USA, 12–14 August 2013.
78. Shchitsyn, Y.; Kartashev, M.; Krivonosova, E.; Olshanskaya, T.; Trushnikov, D. Formation of Structure and Properties of Two-Phase Ti-6Al-4V Alloy during Cold Metal Transfer Additive Deposition with Interpass Forging. *Materials* **2021**, *14*, 4415. [CrossRef]
79. Meng, X.; Min, J.; Sun, Z.; Zhang, W.; Chang, H.; Han, Y. Columnar to Equiaxed Grain Transition of Laser Deposited Ti6Al4V Using Nano-Sized B4C Particles. *Compos. Part B Eng.* **2021**, *212*, 108667. [CrossRef]
80. Olshanskaya, T.; Trushnikov, D.; Dushina, A.; Ganeev, A.; Polyakov, A.; Semenova, I. Microstructure and Properties of the 308LSi Austenitic Steel Produced by Plasma-MIG Deposition Welding with Layer-by-Layer Peening. *Metals* **2022**, *12*, 82. [CrossRef]
81. Shchitsyn, Y.D.; Krivonosova, E.A.; Trushnikov, D.N.; Ol'shanskaya, T.V.; Kartashov, M.F.; Neulybin, S.D. Use of CMT-Surfacing for Additive Formation of Titanium Alloy Workpieces. *Metallurgist* **2020**, *64*, 67–74. [CrossRef]
82. Pouzet, S.; Peyre, P.; Gorny, C.; Castelnau, O.; Baudin, T.; Brisset, F.; Colin, C.; Gadaud, P. Additive Layer Manufacturing of Titanium Matrix Composites Using the Direct Metal Deposition Laser Process. *Mater. Sci. Eng. A* **2016**, *677*, 171–181. [CrossRef]
83. Gu, D.; Wang, Z.; Shen, Y.; Li, Q.; Li, Y. In-Situ TiC Particle Reinforced Ti–Al Matrix Composites: Powder Preparation by Mechanical Alloying and Selective Laser Melting Behavior. *Appl. Surf. Sci.* **2009**, *255*, 9230–9240. [CrossRef]

84. Zhang, Y.; Yu, D.; Zhou, J.; Sun, D. A Review of Dissimilar Welding for Titanium Alloys with Light Alloys. *Metall. Res. Technol.* **2021**, *118*, 213. [CrossRef]
85. Stráský, J.; Janeček, M.; Semenova, I.; Čížek, J.; Bartha, K.; Harcuba, P.; Polyakova, V.; Gatina, S. Microstructure and Lattice Defects in Ultrafine Grained Biomedical α + β and Metastable β Ti Alloys. In *Titanium in Medical and Dental Applications*; Elsevier: Amsterdam, The Netherlands, 2018; pp. 455–475. ISBN 978-0-12-812456-7.
86. Gatina, S.A.; Polyakova, V.V.; Modina, I.M.; Semenova, I.P. Fatigue Behavior and Fracture Features of Ti-15Mo Alloy in β-, (α + β)-, and Ultrafine-Grained Two-Phase States. *Metals* **2023**, *13*, 580. [CrossRef]
87. Gatina, S.A.; Polyakova, V.V.; Polyakov, A.V.; Semenova, I.P. Microstructure and Mechanical Properties of β-Titanium Ti-15Mo Alloy Produced by Combined Processing Including ECAP-Conform and Drawing. *Materials* **2022**, *15*, 8666. [CrossRef]
88. Bartha, K.; Stráský, J.; Barriobero-Vila, P.; Šmilauerová, J.; Doležal, P.; Veselý, J.; Semenova, I.; Polyakova, V.; Janeček, M. In-Situ Investigation of Phase Transformations in Ultra-Fine Grained Ti15Mo Alloy. *J. Alloys Compd.* **2021**, *867*, 159027. [CrossRef]
89. Semenova, I.P.; Shchitsyn, Y.D.; Trushnikov, D.N.; Gareev, A.I.; Polyakov, A.V.; Pesin, M.V. Microstructural Features and Microhardness of the Ti-6Al-4V Alloy Synthesized by Additive Plasma Wire Deposition Welding. *Materials* **2023**, *16*, 941. [CrossRef]
90. Valiev, R.Z.; Islamgaliev, R.K.; Semenova, I.P. Superplasticity in Nanostructured Materials: New Challenges. *Mater. Sci. Eng. A* **2007**, *463*, 2–7. [CrossRef]
91. Medvedev, A.Y.; Astanin, V.V.; Semenova, I.P. The Role of Nanostructural Superplasticity in Blisk Manufacturing. *Nanoindustry* **2019**, *12*, 220–227. (In Russian)